



## Taguchi design-based parametric optimization for sorption Pb(II) ions by acid-treated seed hulls of sunflower

Necla Barlık

Department of Environmental Engineering, Engineering Faculty, Ardahan University, Ardahan, Turkey, Tel.: +90 478 2117500; email: neclabarlik@ardahan.edu.tr

Received 17 March 2023; Accepted 7 June 2023

### ABSTRACT

The seed hulls of sunflower (*Helianthus annuus* L.) treated with  $H_2SO_4$  were used as biosorbent to remove Pb ions from aqueous solutions. The acid-treated biomass was characterized by Brunauer–Emmett–Teller surface area analysis, scanning electron microscopy, Fourier-transform infrared spectroscopy. Optimum conditions for Pb(II) removal from aqueous solutions using the acid-treated biomass was determined with the help of the Taguchi experimental design approach. The results were analysed using a signal-to-noise ratio and analysis of variance. The sorption capacity for the optimum levels of process parameters was  $33.10\text{ mg}\cdot\text{g}^{-1}$ . The initial Pb(II) concentration of the solution and the acid-treated biomass dose was the most contributing factors to the performance with 39.30% and 36.96%, respectively, while the agitation rate was the least contributing factor. The Dubinin–Radushkevich adsorption model estimated the mean sorption free energy to be  $8.639\text{ kJ}\cdot\text{mol}^{-1}$ , with a fit ratio of  $R^2 = 0.968$ . The kinetic model describing the time dependent relationship between Pb(II) ions and the acid-treated biomass with the highest agreement was the pseudo-second-order approach. According to these results, chemisorption was assumed to be the main mechanism controlling Pb(II) ion adsorption onto the treated biosorbent.

*Keywords:* Pb(II) removal; Taguchi design; Isotherm models; Kinetic models; Seed hulls of sunflower

### 1. Introduction

As well as natural ways, lead is also released from many anthropogenic activities, including mining, smelting, coal burning, battery industry waste, automobile exhaust, metal plating, leather tanning and finishing processes, fertilizers, pesticides, gasoline, pigment additives, solder, and fire-arms [1,2]. Lead is a toxic heavy metal that can enter the human body through inhalation and food chain from various sources such as air, water, soil and food. It has been reported that after it is taken into the body, it spreads to various organs with blood cells and poses a risk to the cardiovascular system, central nervous system, kidneys and reproductive system, affects cognitive function, postnatal development and hearing ability in infants and children,

and also causes delays in puberty [3,4]. The World Health Organization (WHO) requires that it should not exceed  $10\text{ }\mu\text{g}\cdot\text{m}^{-3}$  in drinking water [5].

In order to remove Pb ions from wastewater, coagulation [6,7], electrocoagulation [8], membrane separation [9], ion exchange [10,11], adsorption/biosorption [12–14], electro-dialysis [15], oxidation [16] or reduction [17] etc. processes are widely used. The adsorption/biosorption process is a proven technology for the removal of heavy metals [18–21] from aqueous solutions because it is an economical and efficient approach, as well as being environmentally friendly and free of toxic by-products. Both a conventional adsorbent with a relatively high production cost such as activated carbon, as well as graphene oxide, bentonite, biochar and many low-cost organic or inorganic materials and their

modified forms have been used for the removal of heavy metals from aqueous solutions [12–14,22].

For any adsorption process carried out under equilibrium conditions, various parameters such as the initial concentration of the adsorbate, the adsorbent dose, the temperature at which the process is carried out, pH and contact time are very important on the process efficiency. Therefore, these parameters need to be individually optimized for maximum process efficiency. Experimental studies are usually conducted to optimize one parameter level for one factor at a time, as one-factor-at-a-time (OAT or OFAAT) [23,24]. This methodology increases the time and cost required to run tests and also overlooks the interactive effects of process parameters on the process. Taguchi's orthogonal arrays (OAs), based on fractional factorial design, is a methodology that reveals the effects of multiple factors and the potential interactions between these factors with effective time and cost management [25]. This optimization tool, which provides an easy, efficient and systematic approach, has been successfully used in many sorption studies for the removal of dyes [26–28] and heavy metals [29–32] from aqueous solutions.

Googerdchian et al. [31] selected ball milling time, the initial concentration of lead ions, initial pH of the solution and the adsorbent dosage as process parameters in their study investigating the adsorption of Pb(II) ions on nanohydroxyapatite. As a result of the studies carried out using the  $L_{16}$  design array, they reported that the removal efficiency of lead ions mainly depends on the adsorbent dose. In another study, Taguchi experimental optimization approach was used for the adsorption of Pb(II), Cu(II) and Cd(II) ions from aqueous solutions using artichoke as the agro-industrial waste biomass [33]. As controllable factors, pH, temperature, sorbent dosage and initial metal concentration were investigated at three levels in an  $L_9$  array. In a study using the Taguchi design for the optimization of the cadmium adsorption process on deposited silt, the effect of its parameters on the removal efficiency was reported as pH of the solution > stirring time > dose of deposited silt > initial concentration of Cd metal ions [30]. Taguchi method was used for process optimization of Ni(II) removal from wastewater with calcined oyster shell powders. It is discussed the pH, temperature, Ni(II) concentration, adsorbent dose, and contact time as the controllable factors in an  $L_{18}$  orthogonal array. As a result, they found that pH was the parameter that contributed the most for removal efficiency [32].

Agricultural waste-based biosorbents can be pre-treated using different acids ( $\text{HNO}_3$ ,  $\text{HCl}$ ,  $\text{H}_2\text{SO}_4$ ,  $\text{C}_4\text{H}_6\text{O}_6$  and  $\text{C}_2\text{H}_4\text{O}_2\text{S}$ ), bases ( $\text{NaOH}$ ,  $\text{KOH}$ ,  $\text{Ca}(\text{OH})_2$ ) or other chemical compounds ( $\text{Al}_2\text{O}_3$ ,  $\text{Fe}_2\text{O}_4$ ,  $\text{KCl}$ ,  $\text{C}_8\text{H}_4\text{O}_3$  etc), and can be chemically modified. Chemical modification: it is a simple and effective process to improve the adsorptive properties, surface active sites and mechanical strength of the raw biosorbent. The surface of the raw biosorbent treated with acids and bases is oxidized, and depending on the chemical structure of the biosorbent and the modification agent used, it can form functional groups that can increase the sorption capacity [34]. The density and adsorption performance of these functional groups may not always be predictable due to many variables such as the complexity of the natural chemistry of the raw biosorbents, the parameters of

the pre-treatment applied and the oxidation ability of the modification agent used.

In this study, performance of removing Pb(II) ions from aqueous solutions of the sunflower seed hulls treated with  $\text{H}_2\text{SO}_4$  was tested. Taguchi's experimental design approach was used for the optimization of the parameters of the process carried out under equilibrium adsorption conditions. Adsorption isotherm models were applied to the experimental data and kinetics were calculated.

## 2. Materials and methods

### 2.1. Preparation of biosorbent

Agricultural waste biomass consisting of the seed hulls of the sunflower (*Helianthus annuus* L.) plant grown in Pasinler, northeast of Turkey, was used. After the peels were physically weed out, they were washed with distilled water and dried at 60°C for 24 h. They were then ground in a household grinder and treated with  $\text{H}_2\text{SO}_4$ . In a 1 L round reaction vessel, 500 mL of acid solution was added to 100 g of shells and kept in a water bath at 40°C for 24 h, so that the shells were thoroughly wetted with the acid solution. Then, acid and agricultural waste were allowed to react for 2 h at 100°C on a heating plate with magnetic stirrer and temperature control. After cooling to room temperature, it was filtered, washed with double distilled water until pH values were 5.00 and dried at 60°C for 24 h. 1 M (approximately 10% (w/w))  $\text{H}_2\text{SO}_4$  solution was used to activate the shells. The dried activated shells were passed through a no. 30 (600  $\mu\text{m}$ ) sieve.

### 2.2. Characterization of biosorbent

The surface properties and textural structure of raw and activated shells were characterized using several techniques. The morphology and superficial structure were observed by field-emission scanning electron microscopy with a ZEISS, Sigma 300 VP Instrument. Energy-dispersive X-ray analysis (EDX) was used to examine the surface elemental composition before and after adsorption. Surface functional groups of raw and activated shells were investigated using Fourier-transform infrared (FTIR) spectroscopy (BRUKER, Tensor II); the FTIR spectra were recorded in the range 400–4,000  $\text{cm}^{-1}$ . Finally, the surface areas, pore volumes and pore sizes of the adsorbent materials were analysed using the Brunauer–Emmett–Teller (BET) technique with isothermal nitrogen gas ( $\text{N}_2$ ) adsorption on the Micromeritics Brand Gemini VII 2390t device.

### 2.3. Chemicals and reagents

Stock lead solution (1,000  $\text{mg}\cdot\text{L}^{-1}$ ) was prepared by dissolving the calculated mass of Merck grade lead nitrate [ $\text{Pb}(\text{NO}_3)_2$ ] in double distilled water. Then, the stock solution was diluted in certain proportions in accordance with the required concentrations to be used for the experiments. The  $\text{H}_2\text{SO}_4$  used for the activation of agricultural waste was Merck brand with a purity of 95%–97%.  $\text{NaOH}$  and  $\text{HNO}_3$  solutions were used to adjust the initial pH values of Pb(II) solutions. Double distilled water was used for all the experiments.

#### 2.4. Process optimization and statistical analysis

Taguchi's experimental design approach was used for the optimization of the process parameters. Process parameters were determined in accordance with many studies [14,30,31,35] for heavy metal removal from aqueous solutions under equilibrium adsorption conditions. The tests were conducted for the parameter levels given in Table 1 and in accordance with the design matrix given in Table 2. The experiments were repeated two times.

The Taguchi experimental design matrix is a fractional orthogonal design that considers a balanced subset of combinations of all levels of all factors. Orthogonal arrays as a type of general fractional factorial design; it considers all levels of all factors equally and enables the determination of the best combination [25]. Controllable process parameters (factors) considered in this study are  $T$ ; process temperature ( $^{\circ}\text{C}$ ), pH,  $C_0$ ; initial Pb(II) concentration ( $\text{mg}\cdot\text{L}^{-1}$ ),  $t$ ; mixing time (min), agitation rate (rpm), and  $m$ ; the treated biomass dose (the adsorbent dose) ( $\text{g}\cdot\text{L}^{-1}$ ). They are denoted by  $A$ ,  $B$ ,

Table 1

Controllable factors and their levels for the  $L_{16}$  ( $4^2^2$ ) orthogonal array

Factors	Parameters of description	Levels			
		$L_1$	$L_2$	$L_3$	$L_4$
A	$T$ ( $^{\circ}\text{C}$ )	20	25	30	35
B	pH	2	3	4	5
C	$C_0$ ( $\text{mg}\cdot\text{L}^{-1}$ )	80	120	160	200
D	$t$ (min)	30	60	90	120
E	Agitation rate (rpm)	300	600	–	–
F	$m$ ( $\text{g}\cdot\text{L}^{-1}$ )	2	4	–	–

Table 2

Design of experiments using  $L_{16}$  ( $4^2^2$ ) orthogonal array

Run	Factors					
	A	B	C	D	E	F
1	1	1	1	1	1	1
2	1	2	2	2	1	2
3	1	3	3	3	2	1
4	1	4	4	4	2	2
5	2	1	2	3	2	2
6	2	2	1	4	2	1
7	2	3	4	1	1	2
8	2	4	3	2	1	1
9	3	1	3	4	1	2
10	3	2	4	3	1	1
11	3	3	1	2	2	2
12	3	4	2	1	2	1
13	4	1	4	2	2	1
14	4	2	3	1	2	2
15	4	3	2	4	1	1
16	4	4	1	3	1	2

$C$ ,  $D$ ,  $E$ , and  $F$ , respectively. The  $L_{16}$  ( $4^2^2$ ) design matrix was applied at the parameter levels shown in Table 1. The agitation rate and the adsorbent dose were considered at two levels, while other factors were considered at four levels. pH values were chosen to ensure that lead ions are in the form of Pb(II) in aqueous solutions. Preliminary experiments were performed to determine other parameter levels. The sorption experiments were carried out in accordance with the design matrix (Table 2), and the adsorption capacities ( $q_t$ ) were recorded as "response" ( $R$ ).

The methodology uses signal-to-noise ratio (S/N) as a statistical performance measure to analyse experimental results. Depending on the desired response performance in the process, the S/N ratio can change as "nominal better", "smaller better", and "larger better". Since optimum conditions were determined to maximize Pb(II) removal from the aqueous solution, the "larger better" quality characteristic given by Taguchi was calculated [25]:

$$\frac{S}{N} = -10 \times \log \left[ \frac{1}{n} \sum_{i=1}^n \frac{1}{R_i^2} \right] \quad (1)$$

In addition, a statistical analysis of variance (ANOVA) was conducted to show the effects of process parameters on Pb(II) removal efficiency. Minitab 20.3 software was used to create the Taguchi experimental design matrix and evaluate the results.

#### 2.5. Sorption tests

The sorption tests were carried out for optimization, isotherm and kinetic modelling of the process of removing Pb(II) from aqueous solutions with the biomass treated with  $\text{H}_2\text{SO}_4$  under equilibrium adsorption conditions.

The sorption tests were carried out using 100 mL of Pb(II) solution in 250 mL flasks in a shaker adjustable to constant temperature and stirring speed. The necessary amount of the treated biomass was added to the solutions with the initial Pb(II) concentration and initial pH value, and they were shaken for the required time at constant the temperature and the agitation rate. After the mixing time was completed, the solution was centrifuged for solid-liquid separation. The solution was then analysed by atomic absorption spectrometry (PerkinElmer – AAnalyst 400 AAS) to determine the Pb ions concentration. The lead removal capacity  $q_t$  was calculated according to the Eq. (2):

$$q_t = \frac{(C_0 - C_t)V}{M} \quad (2)$$

#### 2.6. Isotherm and kinetic studies

For equilibrium isotherm and kinetic studies, tests were carried out at  $25^{\circ}\text{C}$ . The initial pH of the solutions was adjusted to 5, the treated biosorbent dosage of  $2 \text{ g}\cdot\text{L}^{-1}$  and the agitation rate of 600 rpm. Solutions with different the initial Pb(II) concentrations in the range of  $75\text{--}300 \text{ mg}\cdot\text{L}^{-1}$  were selected for isotherm tests. Equilibrium Pb ions concentrations were analysed in the centrifuged solutions after 120 min.

In tests carried out for kinetic studies, the initial Pb(II) concentration was determined as 200 mg·L<sup>-1</sup>. The tests were carried out for 10 different adsorption times in the range of 5–120 min. At the end of the specified time, the concentrations of Pb ions in the centrifuged solutions were analysed.

The results of the equilibrium ion adsorption tests were compared with the Langmuir, Freundlich, Temkin and Dubinin–Radushkevich isotherm models and the results of the kinetic tests were compared with the pseudo-first-order, pseudo-second-order, Elovich and intraparticle diffusion models. The non-linear and linear forms of these models are given in Table 3. Model parameters were calculated from the slope and cut points obtained from the graph drawings based on linearized equations.

### 3. Results and discussion

#### 3.1. Characterization of biosorbent

##### 3.1.1. BET surface area and porosity

Raw and the treated biomass were characterized in terms of surface properties such as surface area and pore size. Surface area in biosorbents is a microgeometry dependent property of powdered and porous materials and can provide important information about their sorption

properties. It is preferred that the sorbents have a larger specific surface area to provide greater sorption capacity.

The surface area, total pore volume, micropore volume and mean pore diameter of the raw and the treated biomass were determined. The results are shown in Table 4. The BET surface area and total pore volume of the raw biomass are 19.34 m<sup>2</sup>·g<sup>-1</sup> and 18.70 × 10<sup>-3</sup> cm<sup>3</sup>·g<sup>-1</sup>, respectively. Both of these values were reduced by acid treatment. The micropore volume that was not detected in the raw biomass was measured as 8.31 × 10<sup>-4</sup> cm<sup>3</sup>·g<sup>-1</sup> in the treated biomass. The treated and the raw biomass have mesopores (2–50 nm) [36] and their mean pore diameters are close to each other.

In a study on the adsorptive properties of agrifood processing wastes, the surface characterization of citrus waste, artichoke agro-waste and olive mill residue were investigated [37]. Their BET surface areas were recorded as 1.804, 0.913 and 3.727 m<sup>2</sup>·g<sup>-1</sup> for the citrus waste, artichoke agro-waste and olive mill residue, respectively. Also, their total micropore volumes were 0.0019, 0.0015 and 0.0048 cm<sup>3</sup>·g<sup>-1</sup>, respectively.

##### 3.1.2. Scanning electron microscopy observations

Scanning electron microscopy (SEM) was used to determine the morphological differences between the raw, the treated biomass and after Pb(II) adsorption. After all samples

Table 3  
Linear equations and the parameters for isotherm and kinetics models [52]

	Non-linear form	Linear form	Plot
Equilibrium adsorption isotherm models			
Langmuir	$q_e = \frac{q_{ml} K_L C_e}{1 + K_L C_e}$	$\frac{C_e}{q_e} = \frac{1}{q_{ml} K_L} + \frac{C_e}{q_{ml}}$	$C_e/q_e$ vs. $C_e$
Freundlich	$q_e = K_F C_e^{1/n_F}$	$\ln q_e = \ln K_F + \frac{1}{n_F} \ln C_e$	$\ln q_e$ vs. $\ln C_e$
Temkin	$q_e = \left(\frac{RT}{b_T}\right) \ln(K_T C_e)$	$q_e = \left(\frac{RT}{b_T}\right) \ln K_T + \left(\frac{RT}{b_T}\right) \ln C_e$	$q_e$ vs. $\ln C_e$
Dubinin–Radushkevich	$q_e = q_m \exp[-K_D \varepsilon^2]$ $\varepsilon = RT \ln \left(1 + \frac{1}{C_e}\right)$	$\ln q_e = \ln q_m - K_D \varepsilon^2$ $E = \frac{1}{(2K_D)^{1/2}}$	$\ln q_e$ vs. $\varepsilon^2$
Kinetic models			
Pseudo-first-order	$\frac{d(q_t)}{dt} = k_1 (q_e - q_t)$	$\ln(q_e - q_t) = \ln q_e - k_1 t$	$\ln(q_e - q_t)$ vs. $t$
Pseudo-second-order	$\frac{d(q_t)}{dt} = k_2 (q_e - q_t)^2$	$\frac{t}{q_t} = \frac{1}{k_2 q_e^2} + \frac{1}{q_e} t$	$t/q_t$ vs. $t$
Elovich equation	$\frac{d(q_t)}{dt} = \alpha \exp(-\beta q_t)$	$q_t = \frac{1}{\beta} \ln(\alpha\beta) + \frac{1}{\beta} \ln(t)$	$q_t$ vs. $\ln(t)$
Intraparticle diffusion	$q_t = k_t t^{1/2} + C$		$q_t$ vs. $t^{1/2}$

were dried and covered with gold, SEM images were taken at different magnifications between 50x and 10Kx. Fig. 1 shows the differences between the 100x and 5Kx magnified surface images of the raw and the treated biomass. SEM shows a raw vegetative structure of sunflower seed hull powder (Fig. 1a1 and a2) consisting of fine particles that do not have a regular, fixed shape and size. The particles are of various sizes and have a rough appearance on

Table 4  
BET surface area and porosity of the raw and the treated biomass

Property	raw biomass	Treated biomass
BET surface area ( $\text{m}^2 \cdot \text{g}^{-1}$ )	$19.34 \pm 0.29$	$10.87 \pm 0.10$
External surface ( $\text{m}^2 \cdot \text{g}^{-1}$ )	26.46	14.31
Micropore surface area ( $\text{m}^2 \cdot \text{g}^{-1}$ )	Not detected	1.44
Micropore volume ( $\text{cm}^3 \cdot \text{g}^{-1}$ )	Not detected	$8.31 \times 10^{-4}$
Total porous volume ( $\text{cm}^3 \cdot \text{g}^{-1}$ )	$18.70 \times 10^{-3}$	$9.80 \times 10^{-3}$
Pore diameter (nm)	3.86	3.59

the outer surface with many cracked edges and twists. This can be attributed to the presence of impurities spread over the surface [38]. These impurities can be removed by acid treatment as indicated by the morphologies of the biomass. The surface of the acid-treated biomass given in Fig. 1b1 and b2 is cleaner and smoother than the raw one.

Relatively open channels and macropores are seen on the raw biomass surface (Fig. 1a1) but lack pores in its micro geometry (Fig. 1a2). However, after activation with  $\text{H}_2\text{SO}_4$ , micropore formation (Fig. 1b2) is observed in the biomass structure and it has a more closed surface morphology with less impurities as seen in Fig. 1b1. These results are consistent with the results from the BET analysis.

Essentially, treatment with  $\text{H}_2\text{SO}_4$  did not produce a major structural change. The fact that lignin-dependent morphological features of sunflower seed hulls do not change significantly after acid treatment is consistent with the literature [39].

The EDX spectra of the raw, the treated and Pb(II) adsorbed the treated biomass are presented in Fig. 2. The EDX spectrum of the raw biomass (Fig. 2a) agrees with previous studies [35]. The S content of the treated biomass (Fig. 2b) is 12.80 wt.% and the Pb content after the

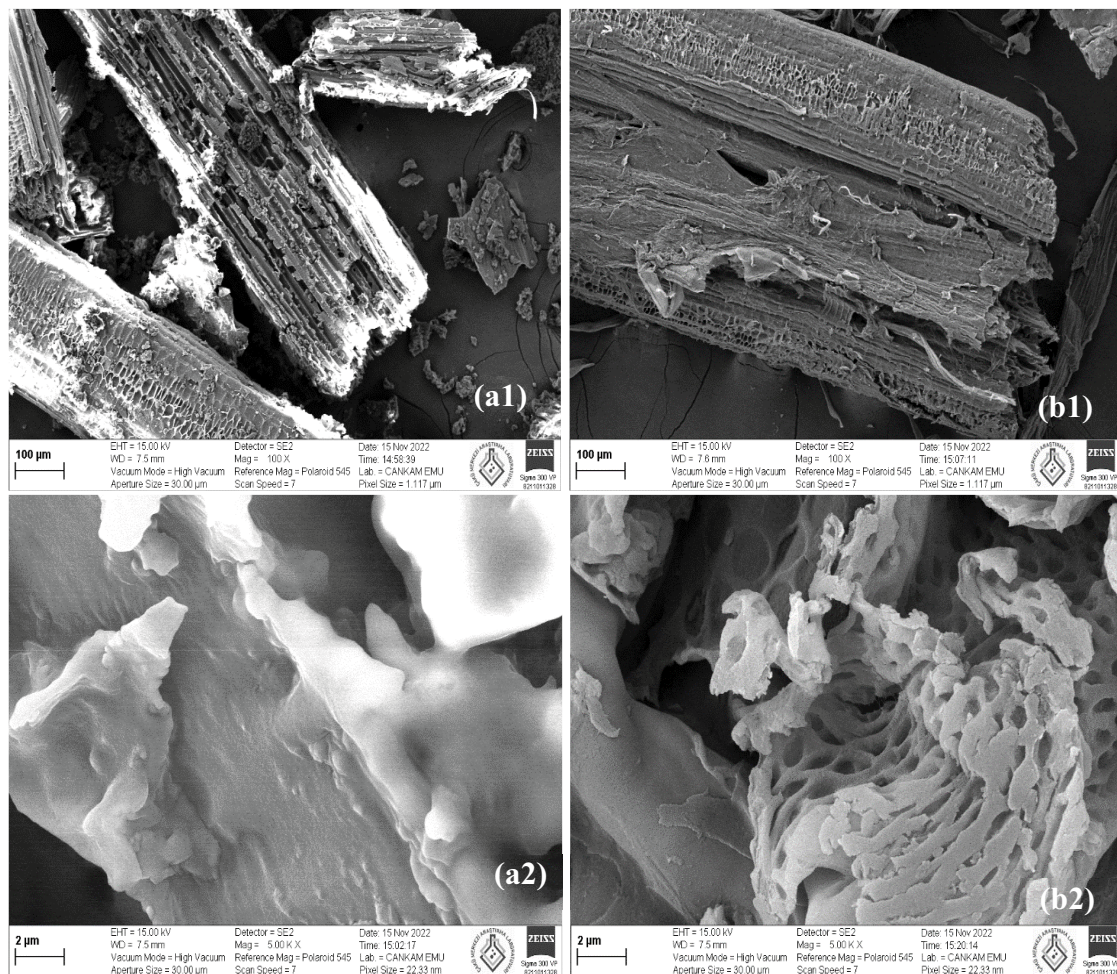


Fig. 1. Scanning electron microscopy images of the raw (a) and the treated (b) biomass (magnification of 100x (a1,b1) and 5Kx (a2,b2)).

adsorption of Pb(II) ions (Fig. 2c) is 32.03 wt.%. It can be seen from Fig. 2 that the physico-chemical properties of the raw biomass become more complex than before after the acid treatment and the adsorption processes.

3.1.3. FTIR analysis

FTIR spectra of the raw, the treated biomass and after the adsorption are shown in Fig. 3. The broad band in the wavelength range of 3,200–3,400  $\text{cm}^{-1}$  are assigned to the presence of hydroxyl stretches of alcohols and phenols [40] in the structure. The -OH group in the raw and the treated structures can be identified at wavenumbers of 3,292 and 3,336  $\text{cm}^{-1}$ , respectively. The treated biomass has lower peak intensities of -OH groups than the raw. For the raw biomass the double peaks at 2,923 and 2,853  $\text{cm}^{-1}$  and for the

treated biomass at 2,919 and 2,853  $\text{cm}^{-1}$  represent symmetric and asymmetric stretching of C-H, respectively, and their bending vibrations are at wavenumbers of 1,366 and 1,317  $\text{cm}^{-1}$  [40,41]. These peaks are mostly are sharply for the raw structure than the treated. After adsorption of Pb ions these peaks shifted to 2,916 and 2,858  $\text{cm}^{-1}$ , respectively.

At a wavenumber range of 1,750–1,500  $\text{cm}^{-1}$ , it has observed for the raw treated biomass in comparison to the treated biomass, sharper peaks. The absorption band at 1,744 and 1,710  $\text{cm}^{-1}$  in the raw biomass spectra and at 1,737 (after the adsorption at 1,734) and 1,713  $\text{cm}^{-1}$  (after the adsorption at 1,717) in the treated biomass spectra may be related to C=O stretching of aldehydes, ketones and carboxylic acids. The peaks are at 1,633 and 1,641. They are due to stretching vibration of C=O [42]. The peaks observed at 1,597  $\text{cm}^{-1}$  in the treated, at 1,536 in the raw could be due to

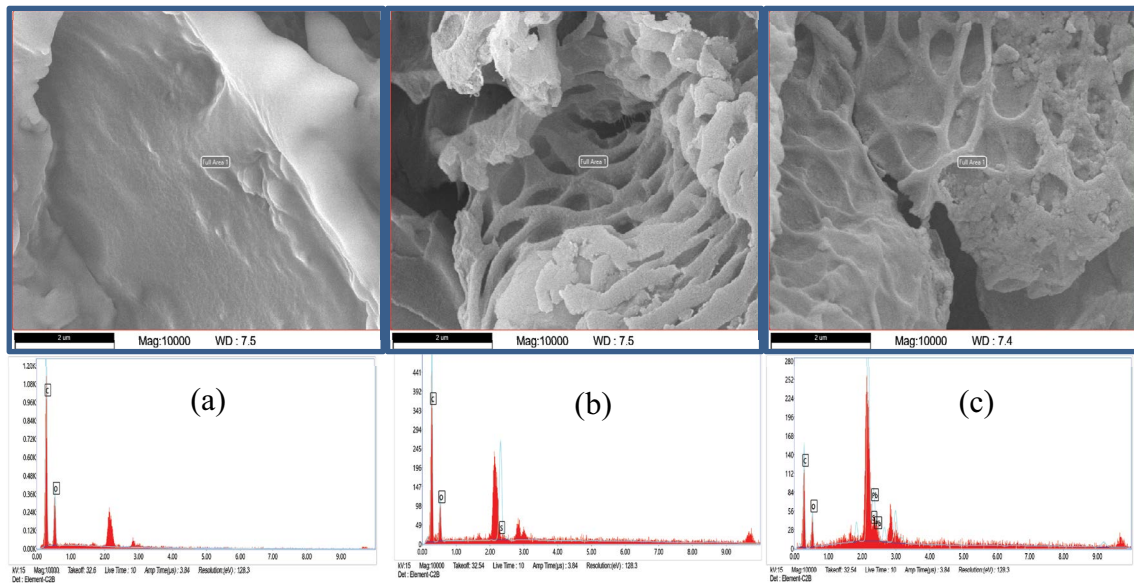


Fig. 2. Scanning electron microscopy images of the raw biomass (a) the treated biomass (b) and the Pb(II) ions loaded the treated biomass (c) with energy-dispersive X-ray spectrum.

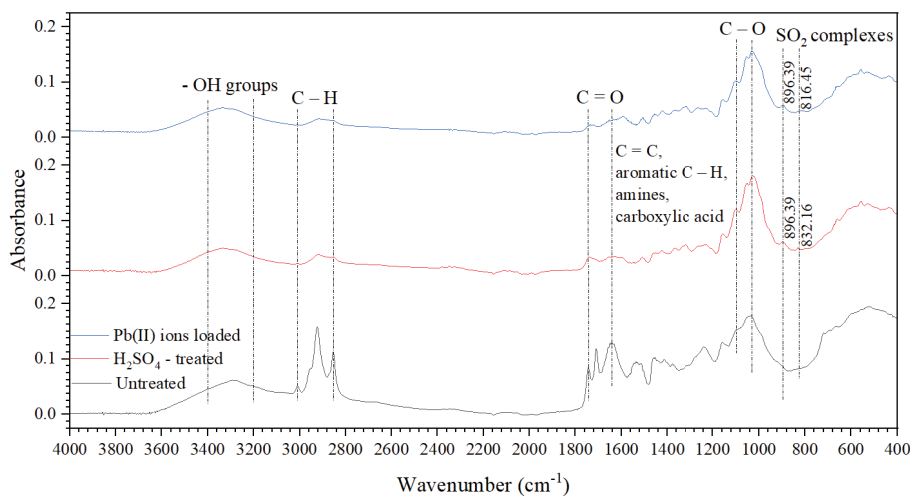


Fig. 3. Fourier-transform infrared spectra of the raw, the treated biomass and Pb(II) ions loaded the treated biomass.

the stretching vibration of C=C and primary amide groups in aromatic rings [40,43]. It has been reported that the wavelength of around 1,510  $\text{cm}^{-1}$  is a constant peak for lignin esters [44]. The band at 1,454  $\text{cm}^{-1}$  in the spectra of the raw biomass may be associated with  $\text{CH}_2$ ,  $\text{CH}_2$ , aromatic rings caused by the bending vibration of C–H and the stretching vibration of aromatics [41]. This band shifted to 1,452  $\text{cm}^{-1}$  for the treated biomass. The width at 1,239  $\text{cm}^{-1}$ , which appears more sharply in the raw biomass, could be due to the vibration of the carboxylic acids.

The band at wavenumber of 1,158  $\text{cm}^{-1}$  are considered to occur due to C–O stretching of lipids and bending of alcohol groups. The band at 1,035  $\text{cm}^{-1}$  for the raw biomass and shifted to at 1,028  $\text{cm}^{-1}$  for the treated biomass is related to primary and secondary alcohols and to stretching of ester groups [41]. After adsorption of Pb(II) this band shifted to 1,029  $\text{cm}^{-1}$ . Also, the spectrum of the treated biomass shows that new absorption bands appear at 896 and 832  $\text{cm}^{-1}$  (after the adsorption at 816  $\text{cm}^{-1}$ ) in the spectrum of the treated sample compared to the raw. These vibrational bands at about 900–800  $\text{cm}^{-1}$  can be assigned to the stretching vibrations of  $\text{SO}_2$  due to sulphur absorption, and the presence of surface  $\text{SO}_2$  complexes [35]. The band at 522  $\text{cm}^{-1}$  for the raw biomass and shifted to at 522  $\text{cm}^{-1}$  for the treated biomass is assigned to halo compounds although this may also be represented to an interaction between metal ions and N-containing bioligands [42].

The FTIR spectra of the treated biomass show appreciable change respect the raw biomass. It is expected that the surfaces of the treated biomass will be cleaned and the organic structure will be charged with protons. As can be seen in Fig. 3, the density of single C–O bonds between 1,100 and 1,000  $\text{cm}^{-1}$  increased relatively after the treatment and the peak sharpened around 1,030  $\text{cm}^{-1}$ . In this case, it can be expected that functional groups such as primary, secondary,

tertiary alcohols and esters will increase. On the other hand, the disappearance of the peaks in the 3,000–2,800  $\text{cm}^{-1}$  and 1,700–1,200  $\text{cm}^{-1}$  bands can be explained that the acids destroyed many bonds in the aliphatic and aromatic compounds in present the raw biomass. Essentially, hydrolysis would be expected to improve sorption by replacing functional groups attached to the raw biomass and forming new functional groups such as carboxyl, carboxylate, and alcohol [45].

### 3.2. Taguchi optimization

The effects of the initial pH of the solution, the initial Pb(II) concentration, the process temperature and time, the agitation rate and adsorbent dose on the removal of Pb(II) from aqueous solutions were investigated using the  $L_{16}$  ( $4^2^2$ ) orthogonal array. The response values ( $q_i$ ) determined from the experiments carried out in accordance with the experimental design matrix (Table 2) followed in the experimental studies are given in Table 5. Each experiment was repeated twice and the average sorption capacity was recorded as the response value. In addition, the values of the S/N ratios calculated with Eq. (2), which are focused as a quality characteristic in the evaluation of experimental results in the Taguchi method, under the ‘larger better’ conditions are also given in Table 5. The S/N ratio was found to be 29.98 and 21.53 with the highest (run 10) and lowest (run 16) ratios, respectively. Again, the mean removal capacity for these runs was 31.57 and 11.93  $\text{mg}\cdot\text{g}^{-1}$ , respectively.

#### 3.2.1. Main effect plot for S/N ratio

According to the larger better-quality characteristic, the optimal level of process parameters is the level corresponding to the largest S/N ratio. The response curves for

Table 5  
Design of experiments using  $L_{16}$  ( $4^2^2$ ) orthogonal array, the removal capacity and the S/N ratio

Run	Parameters						Response ( $q_i$ , $\text{mg}\cdot\text{g}^{-1}$ )		S/N ratio
	$T$ ( $^{\circ}\text{C}$ )	pH	$C_0$ ( $\text{mg}\cdot\text{L}^{-1}$ )	$t$ (min)	Agitation rate (rpm)	$m$ ( $\text{g}\cdot\text{L}^{-1}$ )	$R_1$	$R_2$	
1	20	2	80	30	300	2	12.31	11.83	21.64
2	20	3	120	60	300	4	14.90	14.99	23.49
3	20	4	160	90	600	2	28.56	28.04	29.04
4	20	5	200	120	600	4	20.61	20.66	26.29
5	25	2	120	90	600	4	12.86	11.48	21.71
6	25	3	80	120	600	2	17.93	18.69	25.25
7	25	4	200	30	300	4	22.16	21.88	26.86
8	25	5	160	60	300	2	28.79	29.20	29.25
9	30	2	160	120	300	4	12.31	12.53	21.88
10	30	3	200	90	300	2	31.72	31.41	29.98
11	30	4	80	60	600	4	13.01	12.92	22.26
12	30	5	120	30	600	2	22.11	22.42	26.95
13	35	2	200	60	600	2	22.29	22.13	26.93
14	35	3	160	30	600	4	17.43	17.80	24.92
15	35	4	120	120	300	2	24.51	24.18	27.73
16	35	5	80	90	300	4	12.03	11.82	21.53

the individual effects of Pb(II) adsorption process parameters on sorption capacities ( $q_t$ ) and their corresponding S/N ratios are shown in Fig. 4. The figure also shows the true error bars for the mean  $q_t$  values. The changes in the mean response and the S/N ratios against the levels of the parameters can be seen from these curves. The S/N ratio, the delta and the ranks values for each factor and its levels are given in Table 6.

The delta value for any factor is determined by the difference between the highest and lowest mean S/N ratio. The delta measures the magnitude of the impact and shows its relative impact. Therefore, the larger the delta, the more intense the effect is expected [25]. The rank value allows factors to be defined directly according to the effect size they have.

The removal capacity is strongly influenced by the parameter levels. The biggest factor affecting the S/N ratio was the initial Pb(II) concentration. The agitation rate was seen as the factor with the least impact. The optimum the S/N ratio the value for each factor is indicated in bold in Table 6. Process parameters that maximize optimum Pb ions removal were determined as at the level 2 (25°C) for the temperature, at the level 3 (4) for the initial pH solution, at the level 4 (200 mg·L<sup>-1</sup>) for the initial Pb(II) concentration, at the level 3 (90 min) for the proses time, the level 2 (600 rpm) for the agitation rate, and the level 1 (2 g·L<sup>-1</sup>) for the adsorbent dose. Therefore, the optimum combination of process parameters was  $T_2, pH_3, C_{04}, t_3, agitation_2$  and  $m_1$ .

### 3.2.2. Implementation of ANOVA

ANOVA was conducted to investigate to what extent the process parameters affect the mean removal capacity and to determine the percentage contributions of the parameters at the 95% confidence level. ANOVA analysis is also important for the reliability of the observed results [46].

ANOVA results are given in Table 7. According to the table, the contribution percentage of the errors (0.211%) was much smaller than 50%, which means that the experiments were carried out under controlled conditions [31]. It has been seen that the initial Pb(II) concentration of the solution

and the adsorbent dose have very close values according to the contribution percentages in the adsorption of Pb(II) on the treated biomass. pH follows with an additive ratio of 22.39%. On the other hand, the process temperature, time and the agitation rate have been seen as factors with relatively less effect.

Table 6  
Response table of the S/N ratios for Pb(II) removal (larger is better)

Level	$T$ (°C)	pH	$C_0$ (mg·L <sup>-1</sup> )	$t$ (min)	Agitation rate (rpm)	$m$ (g·L <sup>-1</sup> )
1	25.11	23.04	22.67	25.09	25.29	<b>27.10</b>
2	<b>25.77</b>	25.91	24.97	25.48	<b>25.42</b>	23.62
3	25.27	<b>26.47</b>	26.27	<b>25.56</b>	–	–
4	25.28	26.00	<b>27.52</b>	25.29	–	–
Delta	0.65	3.43	4.85	0.47	0.12	3.48
Rank	4	3	1	5	6	2

Table 7  
Analysis of variance for the means

Source	DOF	Sum of squares	Variance	F-ratio	Contribution (%)
$T$ (°C)	3	0.963	0.321	1.52	0.73
pH	3	29.341	9.781	46.41	22.39
$C_0$ (mg·L <sup>-1</sup> )	3	51.499	17.166	81.45	39.30
$t$ (min)	3	0.536	0.179	0.85	0.41
Agitation rate (rpm)	1	0.062	0.062	0.29	0.05
$m$ (g·L <sup>-1</sup> )	1	48.444	48.444	229.86	36.96
Error	1	0.211	0.211	–	0.16
Total	15	131.056			100.00
$R^2$		0.998			
Adj. $R^2$		0.976			

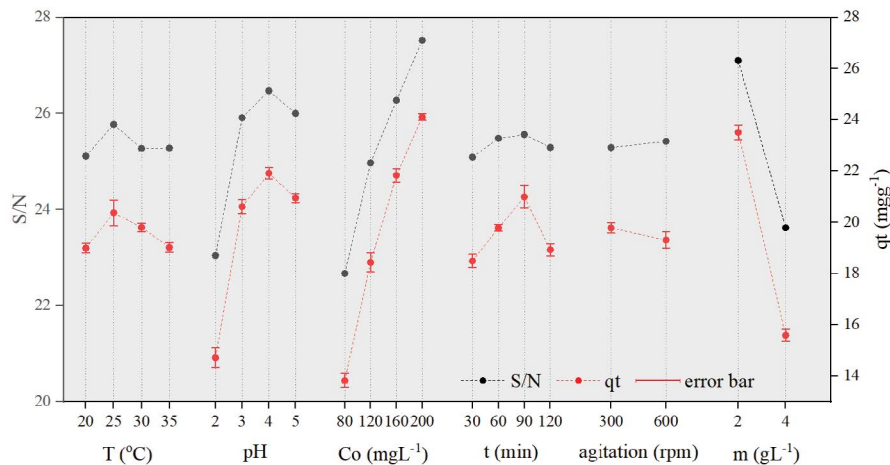


Fig. 4. Main effects of factors on  $q_t$  (with true error bars) and S/N ratio for Pb(II) ion adsorption.

According to Fig. 4, the S/N ratio increased as the initial Pb(II) concentration increased from 80 to 200 mg·L<sup>-1</sup>. According to the larger better-quality characteristic analysis (Table 6) and ANOVA results (Table 7), the most important factor contributing to the removal performance of Pb(II) ions was the initial Pb(II) concentration. These results are agreed with similar studies in the literature [33]. The difference in Pb ions concentration between the biomass and solution is used as the driving force for transport from the bulk solution to the treated biomass surface. At high Pb(II) ion concentrations in the bulk, it is expected that the sorption performance will increase due to the easier and more convenient transport of these ions to the active sites on the biomass, but when the initial concentration is excessively high, the active sites will saturate faster, which prevents further ion uptake [47].

Adsorbent dosage is another important factor that directly affects the metal removal capacity of biosorbents from aqueous solutions. According to the results given in Tables 6 and 7, the dosage of treated biomass significantly affected the removal of Pb(II) ions from the aqueous solution. Despite the increased dosage of treated biomass, the Pb(II) adsorption capacity and the decrease in the S/N ratio (Fig. 4) can be explained by particle aggregation. Since the increase in the amount of biosorbent provides more available adsorption sites for the metal ions in the solution, the amount of biosorbent is generally considered as a parameter that increases the adsorption capacity. However, since excessive biosorbent dosage will lead to particle agglomeration, it may play a role that reduces the active surfaces and therefore reduces the adsorption capacity [48]. Similarly, in the optimization study of Srivastava et al. [29], regarding the biosorption of Pb(II) ions on artichoke agro-waste biomass, higher S/N ratios were observed at low biomass dosages.

In the removal of heavy metals from aqueous solutions, the pH values of the solutions are a basic operational parameter that affects the process, as it can affect the surface charge of the adsorbent, the distribution of metal species and the functional group separation in the active sites [49]. Edokpayi et al. [50], who studied lead adsorption on the mucilage leaves of the *Dicerocaryum eriocarpum* plant, stated that the Pb(II) removal capacity increased from solutions up to the initial pH value of 4, and the capacity began to decrease after this value.

As a result of the optimization experiments, it was observed that the larger is better quality characteristic reached the largest S/N ratio (Fig. 4) for the temperature value of 25°C. After this value, it is seen that the adsorption removal efficiency and S/N ratio decrease at 30°C and 35°C

process temperatures. In an adsorption process, temperature is an important parameter that affects both the solubility and the interaction between the ion/molecule to be removed from the solution and the sorbent. This effect may vary depending on whether the process is endothermic or exothermic. In the literature, there are studies in which the adsorption of heavy metals by carbon-based compounds is exothermic, thus increasing the temperature causes a decrease in the adsorption capacity [47,51].

The parameter with the lowest effect on Pb ions treated biomass was the agitation rate. However, the S/N ratio was observed to be relatively larger for the 600 rpm the agitation rate level. It can be said that it provides a homogeneous bulk solution in terms of the agitation rate levels chosen in the process, and appropriately disperses Pb(II) and treated biomass [43].

### 3.2.3. Confirmation experiments

In the Taguchi process optimization approach, validation experiments should be performed for optimum quality characteristics. Two validation experiments were performed at optimum conditions estimated from the S/N ratio results. The mean S/N value was determined and compared with the predicted values. According to the results given in Table 5, the optimal  $q_e$  and S/N ratios calculated with the software were 32.46 mg·g<sup>-1</sup> and 31.05, respectively. In the average results obtained from the confirmation experiments given in Table 8, these values were observed as 33.10 mg·g<sup>-1</sup> and 30.40, respectively, and both results were within the 95% confidence and prediction intervals. This indicates a good agreement between expected and observed results under optimized conditions and that the experimental results are reproducible.

When the predicted results of the linear regression model based on all the tests included in the L<sub>16</sub> design matrix are compared with the observed results, this agreement is seen. All observed and predicted results in the model graph given in Fig. 5 can be defined with a line with intercept  $0 \pm 0.4323$  and slope  $1 \pm 0.0210$  ( $R^2 = 0.993$ ) within the 95% confidence interval.

Certainly, these optimal values are valid for the specified ranges of process parameters and any extrapolation or interpolation needs to be verified by additional experiments to be carried out separately.

### 3.3. Adsorption isotherms and kinetics

The correlation between the concentration of Pb ions in solution at equilibrium and the concentration of Pb ions

Table 8  
Confirmation experiments of the process optimization

Optimal levels of process parameters	Predicted optimal values	Average of confirmation tests	Confidence intervals (95%)
$T_2, pH_3, C_{04}, t_3, agitation_2, m_1$	$q_e$ (mg·g <sup>-1</sup> )	32.46	CI: 7.95; 56.97 PI: -2.77; 67.69
	S/N	31.05	CI: 25.51; 36.56 PI: 23.09; 38.98

in the treated biomass was determined using adsorption isotherms. Langmuir, Freundlich, Temkin and Dubinin–Radushkevich equilibrium adsorption isotherm models were used to evaluate the adsorption equilibrium.

While the Langmuir isotherm model accepts that adsorption occurs at one molecular thickness and at certain active localized regions of the adsorbent, the Freundlich isotherm describes the monolayer adsorption model when there is chemisorption, and the multilayer

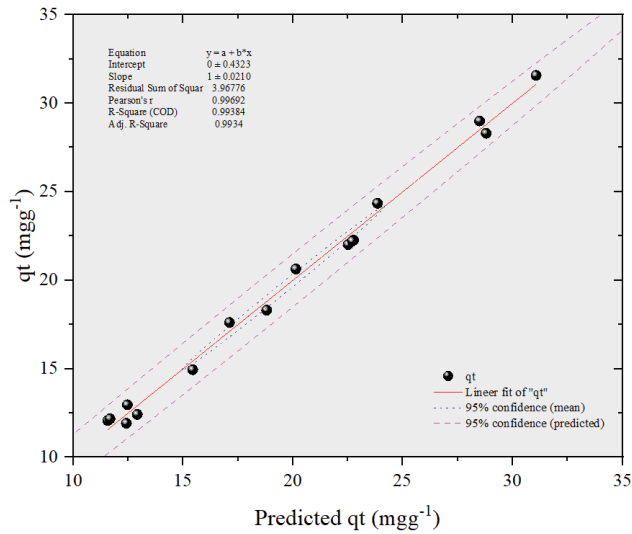


Fig. 5. Linear regression model compared with between observed (mean) and predicted results at 95% confidence interval for Pb(II) ion adsorption.

Table 9

Estimated parameters of isotherm and kinetic models for the adsorption of Pb ions onto the treated biomass

	Intercept	Slope	Parameters	R-square	Adj. R-square
Equilibrium adsorption isotherm models					
Langmuir	0.359	0.040	$q_{mL}$ $K_L$	0.999	0.998
Freundlich	1.106	0.122	$n_f$ $K_f$	0.988	0.986
Temkin	10.961	2.490	$b_T$ $K_T$	0.995	0.994
Dubinin–Radushkevich	3.177	−0.007	$q_m$ $K_D$ $E$	0.968	0.962
Kinetic models					
Pseudo-first-order	3.302	−0.039	$k_1$ $q_e$	0.968	0.964
Pseudo-second-order	0.931	0.028	$k_2$ $q_e$	0.988	0.987
Elovich equation	−9.381	7.844	A B	0.982	0.979
Intraparticle diffusion	0.241	2.760	$K_D$ C	0.938	0.930

adsorption model when there is physiosorption [52]. Unlike the Langmuir and Freundlich isotherm models, the Temkin isotherm model considers the adsorbent–adsorbate interaction. The Temkin isotherm, ignoring very high and low concentration values, assumes a uniform distribution of binding energies [13]. The Dubinin–Radushkevich isotherm model, based on Polanyi theory, considers the structure of the pores in the adsorbent and is used in heterogeneous environments. The mean sorption free energy ( $E$ ) value obtained from this model indicates whether the adsorption process is chemical ( $8 < E < 16 \text{ kJ}\cdot\text{mol}^{-1}$ ) or physical ( $E < 8 \text{ kJ}\cdot\text{mol}^{-1}$ ) [52,53].

The coefficients and degrees of fit found from the linearized equation graphs drawn (in the supplementary file, Fig. 1) for these models are given in Table 9. According to the R-square values, the Langmuir model is the isotherm model with the highest compatibility. This was followed by Temkin, Freundlich and Dubinin–Radushkevich models, respectively. The observed and the estimated values from the isotherm models and their residuals are given in Fig. 6.

The process can be considered as a chemisorption, especially since the experimental results show the highest agreement with the Langmuir isotherm and the mean sorption free energy ( $8.639 \text{ kJ}\cdot\text{mol}^{-1}$ ) calculated from the Dubinin–Radushkevich isotherm model is in the range of  $8 < E < 16 \text{ kJ}\cdot\text{mol}^{-1}$ .

adsorption kinetics can show the relationship between Pb(II) ions and the treated biomass as depend of time. For this purpose, the widely used pseudo-first-order model, pseudo-second-order model, Elovich model and intraparticle diffusion model have been examined. The linearized equation graphs drawn for these models are given in the supplementary file Fig. 2. The coefficients found and the

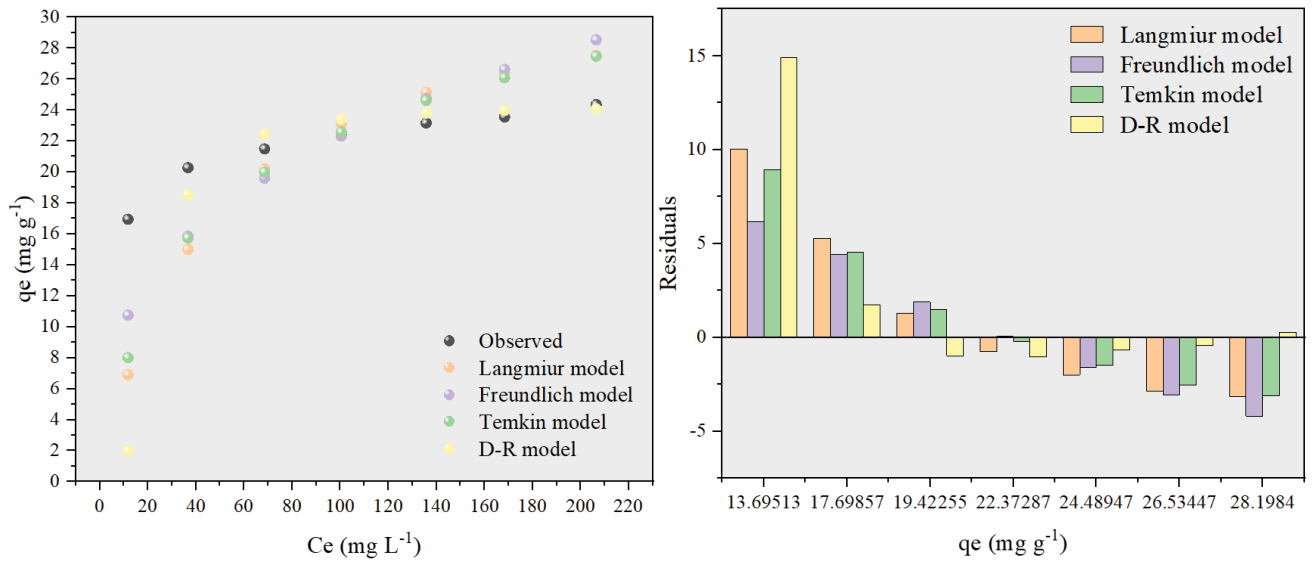


Fig. 6. The observed and the predicted values from the isotherm models (a) and the residues (b) for Pb(II) ions adsorption on the treated biomass.

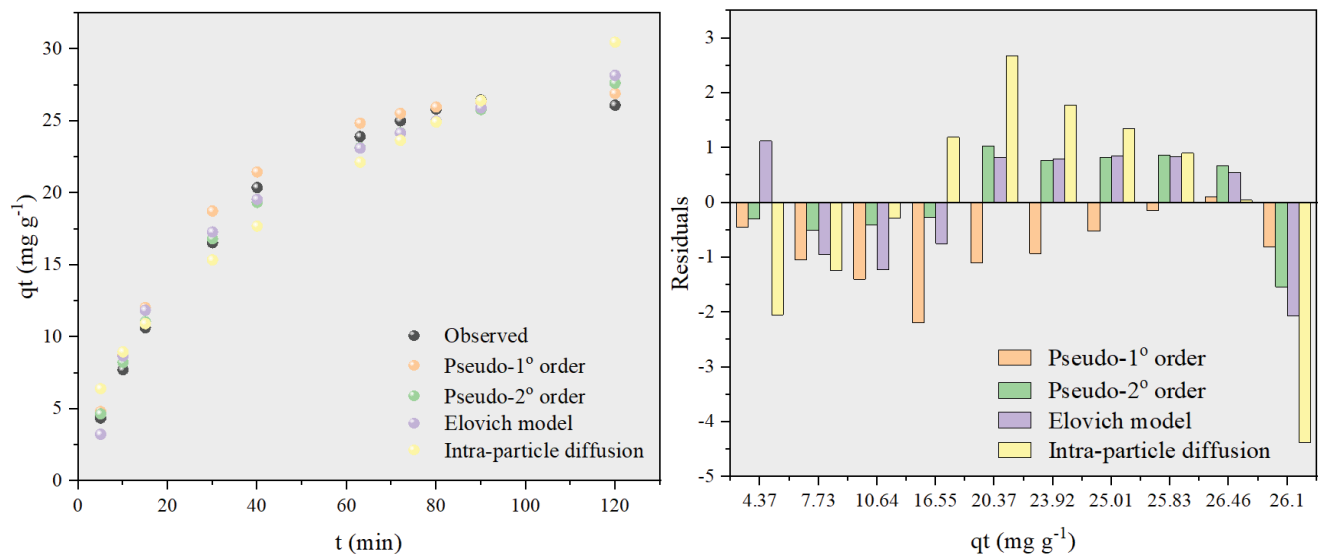


Fig. 7. The observed and the predicted values from the kinetic models (a) and the residues (b) for Pb(II) ions adsorption on the treated biomass.

degree of fit are given in Table 9, and the observed and the estimated values from the models and their residuals are given in Fig. 7.

The results show that the pseudo-second-order model is better fitted because there is a high agreement (0.988) between the predicted equilibrium capacities and the experimentally observed equilibrium capacities, and relatively lower mean relative errors were calculated. Experimental results show the second highest correlation with the Elovich equation. This was followed by the pseudo-first-order model.

Pseudo-first-order and pseudo-second-order models are adsorption – reaction models [52]. The pseudo-first-order model based on Lagergren's kinetics defines the adsorption process as a physio-sorption, while the pseudo-second-

order model defines adsorption as a chemisorption process. The Elovich equation does not predict any precise mechanism, but is useful in describing adsorption on heterogeneous adsorbents such as treated sunflower seed hull. The applicability of the Elovich equation shows that the adsorption of Pb(II) on the treated biomass is predominantly of a chemical nature [54].

The intraparticle diffusion model follows the Weber–Morris model and explains pore diffusion in adsorption processes [13,55]. Experimental results provided the lowest agreement with the intraparticle diffusion model with a correlation coefficient of about 0.94.

In fact, due to the larger size of the liquid molecules, the adsorbents used for the adsorptive removal of metal

Table 10  
Comparison of the maximum adsorption capacity of Pb(II) ions by various biosorbent

Biomass	Treatment	Adsorption capacity (mg·g <sup>-1</sup> )	References
<i>Melia azedarach</i> L. leaves	NaOH	35.1	[57]
	HCl	28.5	
Peanut shell activated carbon	HNO <sub>3</sub>	35.5	[58]
Tea factory waste	No treatment	22.1	[59]
Sporopollenin	HNO <sub>3</sub>	6.1	[60]
Peels of banana	No treatment	5.7	[61]
Walnut shell	No treatment	9.9	[62]
<i>Dicerocaryum eriocarpum</i>	No treatment	41.5	[51]
Mango seed integuments	NaOH	49.9	[63]
<i>Caryota urens</i> seeds carbon	HNO <sub>3</sub>	42.9	[64]
Olive tree pruning	No treatment	27.1	[42]
Seed hulls of sunflower	H <sub>2</sub> SO <sub>4</sub>	33.1	This study

ions from the liquid phase should predominantly have mesopores in their structure [56]. Acid treatment caused the formation of new micropores in the structure of the raw biomass, but did not cause a significant change on the total volume and surface area of the mesopores. As such, the results can be considered to be consistent with the BET analysis results.

For the adsorption of Pb(II) ions, a maximum adsorption capacity of 31.10 mg·g<sup>-1</sup> was obtained in this study. A comparison of the adsorption capacity of the acid-treated sunflower seed hulls and the capacities of some other biomass-based biosorbents is presented in Table 10. The sunflower seed husks can be considered as a potential biosorbent for Pb(II) removal in water and wastewater, as it is a light, brittle and easily processable material and has a higher adsorption capacity than many biosorbents presented in the table.

#### 4. Conclusions

The use of lignocellulosic biomass (raw or modified) obtained from agricultural wastes as an environmentally friendly alternative sorbent for the removal of heavy metals from aqueous solutions has been studied in many studies and continues to be investigated. In this study, sunflower seed hulls, an agricultural industry waste biomass, were modified by treatment with H<sub>2</sub>SO<sub>4</sub> and showed that the treated biomass could be an effective biosorbent for removal of Pb(II) ions from aqueous solutions. The FTIR spectrum and the SEM images showed that acid treatment removed impurities from the raw structure of agricultural waste, consisting of groups such as C–H, C=O, C–C, aromatic C–H and amine.

Taguchi experimental optimization design and ANOVA analysis proved to be a reliable tool to examine the effects of the solution initial pH, the initial Pb ions concentration, the process temperature and time, the agitation rate, and the biomass dosage on the adsorptive removal of lead ions by the treated biomass. Under optimum operating conditions, the treated biomass showed the adsorption capacity of 33.10 mg·g<sup>-1</sup> for removal of Pb(II) ions. With  $q_t$  as response,

all factors considered in the experimental design are statistically significant at the 95% confidence level.

The Langmuir model showed the highest agreement among the four equilibrium adsorption isotherm models studied. According to the Dubinin–Radushkevich equilibrium adsorption model, the mean sorption free energy is greater than 8 kJ·mol<sup>-1</sup>, and also the pseudo-second-order kinetic model was the best kinetic model to explain the sorption behaviour of Pb(II) ions. For these reasons, the process of adsorption of Pb(II) ions onto the treated biomass can be a chemisorption.

These results show that biomass obtained from the acid-modification of the sunflower seed hull, which is locally available almost free of charge, may be a suitable alternative for the removal of Pb(II) ions from aqueous solutions.

#### Symbols

$b_T$	–	Temkin isotherm constant, J·mol <sup>-1</sup>
$C_0$	–	Initial lead concentrations in the aqueous solutions, mg·L <sup>-1</sup>
$C_e$	–	Lead concentrations in the aqueous solutions at equilibrium, mg·L <sup>-1</sup>
$C_t$	–	Lead concentrations in the aqueous solutions at time, mg·L <sup>-1</sup>
CI	–	Confidence interval
PI	–	Prediction interval
$E$	–	Mean sorption free energy from Dubinin–Radushkevich isotherm, J·mol <sup>-1</sup>
$k_1$	–	Pseudo-first-order rate constant, min <sup>-1</sup>
$k_2$	–	Pseudo-second-order rate constant, g·mg <sup>-1</sup> ·min <sup>-1</sup>
$k_i$	–	Intraparticle diffusion rate constant, mg·g <sup>-1</sup> ·min <sup>-1/2</sup>
$K_L$	–	Langmuir equilibrium constant, L·mg <sup>-1</sup>
$K_F$	–	Freundlich equilibrium constant, mg <sup>1-c</sup> ·L <sup>c</sup> ·g <sup>-1</sup> (c: 1/ $n_F$ )
$K_T$	–	Temkin equilibrium constant, L·mg <sup>-1</sup>
$K_D$	–	Dubinin–Radushkevich isotherm constant, mol <sup>2</sup> ·J <sup>-2</sup>
$M$	–	Mass of the treated biomass, g
$n_F$	–	Heterogeneity factor from Freundlich isotherm equation

$n$	—	Total number of experiments for Taguchi design
$q_e$	—	Adsorption capacity at equilibrium, $\text{mg}\cdot\text{g}^{-1}$
$q_m$	—	Dubinin–Radushkevich isotherm saturation capacity, $\text{mg}\cdot\text{g}^{-1}$
$q_{mL}$	—	Langmuir constant for monolayer capacity, $\text{mg}\cdot\text{g}^{-1}$
$q_t$	—	Adsorption capacity at time, $\text{mg}\cdot\text{g}^{-1}$
$R$	—	Universal gas constant, $8.314 \text{ J}\cdot\text{mol}^{-1}\cdot\text{K}^{-1}$
$T$	—	Temperature, $^{\circ}\text{C}$
$t$	—	Adsorption time, min
$V$	—	Aqueous volume of solution, L
$\alpha$	—	Elovich constant, $\text{g}\cdot\text{mg}^{-1}$
$\beta$	—	Initial adsorption rate, $\text{mg}\cdot\text{g}^{-1}\cdot\text{min}^{-1}$
$\varepsilon$	—	Adsorption potential from Dubinin–Radushkevich isotherm

### Abbreviations

D–R	—	Dubinin–Radushkevich
DOF	—	Degrees of freedom
$S/N_{LB}$	—	Signal-to-noise ratio for “larger better”

### References

- A. Kushwaha, N. Hans, S. Kumar, R. Rani, A critical review on speciation, mobilization and toxicity of lead in soil-microbe-plant system and bioremediation strategies, *Ecotoxicol. Environ. Saf.*, 147 (2018) 1035–1045.
- H. Cheng, Y. Hu, Lead (Pb) isotopic fingerprinting and its applications in lead pollution studies in China: a review, *Environ. Pollut.*, 157 (2010) 1134–1146.
- A. Kumar, A. Kumar, M.M.S. Cabral-Pinto, A.K. Chaturvedi, A.A. Shabnam, G. Subrahmanyam, R. Mondal, D.K. Gupta, S.K. Malyan, S.S. Kumar, S.A. Khan, K.K. Yadav, Lead toxicity: health hazards, influence on food chain, and sustainable remediation approaches, *Int. J. Environ. Res. Public Health*, 17 (2020) 2179, doi: 10.3390/ijerph17072179.
- R. Pervin, M.A. Hossain, D. Debnath, M.A. Bhuiyan, in: D. Bagchi, M. Bagchi, *Metal Toxicology Handbook*, CRC Press, Boca Raton, 2020.
- World Health Organization, *Guidelines for Drinking-Water Quality: Fourth Edition Incorporating the First Addendum*, Licence: CC BY-NC-SA 3.0 IGO, Geneva, 2017.
- F.M. Pang, P. Kumar, T.T. Teng, A.K.M. Omar, K.L. Wasewar, Removal of lead, zinc and iron by coagulation–flocculation, *J. Taiwan Inst. Chem. Eng.*, 42 (2011) 809–815.
- C. Suo, D. Xu, R. Yuan, B. Zhou, Synchronous removal of Cd(II), Pb(II), and Cu(II) by coagulation in the presence of polymeric ferric sulfate, *Desal. Water Treat.*, 195 (2020) 421–434.
- M.K. Khosa, M.A. Jamal, A. Hussain, M. Muneer, K.M. Zia, S. Hafeez, Efficiency of aluminum and iron electrodes for the removal of heavy metals [(Ni(II), Pb(II), Cd(II)] by electrocoagulation method, *J. Korean Chem. Soc.*, 57 (2013) 316–321.
- N. Abdullah, N. Yusof, W.J. Lau, A.F. Ismail, Recent trends of heavy metal removal from water/wastewater by membrane technologies, *Ind. Eng. Chem. Res.*, 76 (2019) 17–38.
- S.N. Katariya, S. Kumar, R.B. Yadav, Kinetics and thermodynamics of removal of metal ions using EDTA-modified cation ion exchange resin, *Desal. Water Treat.*, 233 (2021) 133–149.
- D. Egrani, M.T. Late, N. Wessey, N.R. Poyi, S. Acharjee, Synthesis and characterization of kaolinite coated with copper oxide and its effect on the removal of aqueous lead(II) ions, *Appl. Water Sci.*, 9 (2019) 109, doi: 10.1007/s13201-019-0989-6.
- H. Khurshid, M.R.U. Mustafa, M.H. Isa, Adsorption of chromium, copper, lead and mercury ions from aqueous solution using bio and nano adsorbents: a review of recent trends in the application of AC, BC, nZVI and MXene, *Environ. Res.*, 212 (2022) 113138, doi: 10.1016/j.envres.2022.113138.
- T. Liu, Y. Lawluy, Y. Shi, J.O. Ighalo, Y. He, Y. Zhang, Y. Pow-Seng, Adsorption of cadmium and lead from aqueous solution using modified biochar: a review, *J. Environ. Chem. Eng.*, 10 (2022) 106502, doi: 10.1016/j.jece.2021.106502.
- M.N. Sahmoune, Evaluation of thermodynamic parameters for adsorption of heavy metals by green adsorbents, *Environ. Chem. Lett.*, 17 (2019) 697–704.
- X. Wang, J. Feng, Z. Ma, J. Li, D. Xu, X. Wang, Y. Sun, X. Gao, J. Gao, Application of response surface methodology for modeling and optimization of lead (Pb(II)) removal from seaweed extracts via electro dialysis, *Desal. Water Treat.*, 179 (2020) 280–287.
- W. Pan, C. Pan, Y. Bae, D. Giammar, Role of manganese in accelerating the oxidation of pb(ii) carbonate solids to Pb(IV) oxide at drinking water conditions, *Environ. Sci. Technol.*, 53 (2019) 6699–6707.
- J. Zhang, Y. Li, X. Xie, W. Zhu, X. Meng, Fate of adsorbed Pb(II) on graphene oxide under variable redox potential controlled by electrochemical method, *J. Hazard. Mater.*, 367 (2019) 152–159.
- M. Rosique, J.M. Angosto, E. Guibal, M.J. Roca, J.A. Fernández-López, Factorial design methodological approach for enhanced cadmium ions bioremoval by *Opuntia* biomass, *CLEAN – Soil Air Water*, 44 (2016) 959–966.
- A.H. Sulaymon, S.E. Ebrahim, S.M. Abdullah, T.J. Al-Musawi, Removal of lead, cadmium, and mercury ions using biosorption, *Desal. Water Treat.*, 24 (2010) 344–352.
- A. Almasi, F. Navazeshkha, S.A. Mousavi, Biosorption of lead from aqueous solution onto *Nasturtium officinale*: performance and modeling, *Desal. Water Treat.*, 65 (2017) 443–450.
- R. Flouty, J. El-Khoury, E. Maatouk, A. El-Samrani, Optimization of Cu and Pb biosorption by *Aphanizomenon ovalisporum* using Taguchi approach: kinetics and equilibrium modeling, *Desal. Water Treat.*, 155 (2019) 259–271.
- F. Fu, Q. Wang, Removal of heavy metal ions from wastewaters: a review, *J. Environ. Manage.*, 92 (2011) 407–418.
- S. Razavi, H.V. Gupta, What do we mean by sensitivity analysis? the need for comprehensive characterization of “global” sensitivity in earth and environmental systems models, *Water Resour. Res.*, 51 (2015) 3070–3092.
- A. Saltelli, P. Annoni, How to avoid a perfunctory sensitivity analysis, *Environ. Modell. Software*, 25 (2010) 1508–1517.
- G. Taguchi, *Introduction to Quality Engineering: Designing Quality into Products and Processes*, Asian Productivity Organization, Tokyo, 1986.
- N. Berkane, S. Meziane, S. Aziri, Optimization of Congo red removal from aqueous solution using Taguchi experimental design, *Sep. Sci. Technol.*, 55 (2020) 278–288.
- A.S. Yusuff, O.A. Ajayi, L.T. Popoola, Application of Taguchi design approach to parametric optimization of adsorption of crystal violet dye by activated carbon from poultry litter, *Sci. Afr.*, 13 (2021) e00850, doi: 10.1016/j.sciaf.2021.e00850.
- P.C. Bhomick, A. Supong, M. Baruah, C. Pongener, C. Gogoi, D. Sinha, Alizarin Red S adsorption onto biomass-based activated carbon: optimization of adsorption process parameters using Taguchi experimental design, *Int. J. Environ. Sci. Technol.*, 17 (2020) 1137–1148.
- V.C. Srivastava, I.D. Mall, I.M. Mishra, Optimization of parameters for adsorption of metal ions onto rice husk ash using Taguchi’s experimental design methodology, *Chem. Eng. J.*, 140 (2008) 136–144.
- S.R. Korake, P.D. Jadhao, Investigation of Taguchi optimization, equilibrium isotherms, and kinetic modeling for cadmium adsorption onto deposited silt, *Heliyon*, 7 (2021) e05755, doi: 10.1016/j.heliyon.2020.e05755.
- F. Googerdchian, A. Moheb, R. Emadi, M. Asgari, Optimization of Pb(II) ions adsorption on nanohydroxyapatite adsorbents by applying Taguchi method, *J. Hazard. Mater.*, 349 (2018) 186–194.
- H.Y. Yen, J.Y. Li, Process optimization for Ni(II) removal from wastewater by calcined oyster shell powders using Taguchi method, *J. Environ. Manage.*, 161 (2015) 344–349.

- [33] J.A. Fernández-López, J.M. Angosto, M.J. Roca, M.D. Miñarro, Taguchi design-based enhancement of heavy metals bio-removal by agroindustrial waste biomass from artichoke, *Sci. Total Environ.*, 653 (2019) 55–63.
- [34] H.I. Syeda, I. Sultan, K.S. Razavi, P.S. Yap, Biosorption of heavy metals from aqueous solution by various chemically modified agricultural wastes: a review, *J. Water Process Eng.*, 46 (2022) 102446, doi: 10.1016/j.jwpe.2021.102446.
- [35] S. Pap, V. Bezanovic, J. Radonic, A. Babic, S. Saric, D. Adamovic, M.T. Sekulic, Synthesis of highly-efficient functionalized biochars from fruit industry waste biomass for the removal of chromium and lead, *J. Mol. Liq.*, 268 (2018) 315–325.
- [36] A. Threepanich, P. Praipipat, Powdered and beaded lemon peels-doped iron(III) oxide-hydroxide materials for lead removal applications: synthesis, characterizations, and lead adsorption studies, *J. Environ. Chem. Eng.*, 9 (2021) 106007, doi: 10.1016/j.jece.2021.106007.
- [37] J.A. Fernández-López, M.D. Miñarro, J.M. Angosto, J. Fernández-Lledó, J.M. Obón, Adsorptive and surface characterization of mediterranean agrifood processing wastes: prospection for pesticide removal, *Agronomy*, 561 (2021) 2–17.
- [38] M. Mariana, F. Mulana, L. Juniar, D. Fathira, R. Safitri, S. Muchtar, M.R. Bilad, A.H.M. Shariff, N. Huda, Development of biosorbent derived from the endocarp waste of gayo coffee for lead removal in liquid wastewater—effects of chemical activators, *Sustainability*, 13 (2021) 3050, doi: 10.3390/su13063050.
- [39] J.J. Alvear-Daza, A. Cánneva, J.A. Donadelli, M. Manrique-Holguín, J.A. Rengifo-Herrera, L.R. Pizzio, Removal of diclofenac and ibuprofen on mesoporous activated carbon from agro-industrial wastes prepared by optimized synthesis employing a central composite design, *Biomass Convers. Biorefin.*, (2022), doi: 10.1007/s13399-021-02227-w.
- [40] D.L. Pavia, G.M. Lampman, G.S. Kriz, J.R. Vyvyan, *Introduction to Spectroscopy*, Cengage Learning, USA, 2013.
- [41] R.N. Oliveira, M.C. Mancini, F.C. Salles de Oliveira, T.M. Passos, B.Q.R.M. de S. Moreira Thiré, G.B. McGuinness, FTIR analysis and quantification of phenols and flavonoids of five commercially available plants extracts used in wound healing, *Rev. Matéria*, 21 (2016) 767–779.
- [42] M. Calero, A. Pérez, G. Blázquez, A. Ronda, M.A. Martín-Lara, Characterization of chemically modified biosorbents from olive tree pruning for the biosorption of lead, *Ecol. Eng.*, 58 (2013) 344–354.
- [43] B. Hayoun, M. Bourouina, M. Pazos, A.M. Sanromán, S. Bourouina-Bacha, Equilibrium study, modeling and optimization of model drug adsorption process by sunflower seed shells, *Appl. Sci.*, 10 (2020) 3271, doi: 10.3390/app10093271.
- [44] B. Southichak, K. Nakano, M. Nomura, N. Chiba, O. Nishimura, *Phragmites australis*: a novel biosorbent for the removal of heavy metals from aqueous solution, *Water Res.*, 40 (2006) 2295–2302.
- [45] A.E. Ofomaja, E.B. Naidoo, Biosorption of copper from aqueous solution by chemically activated pine cone: a kinetic study, *Chem. Eng. J.*, 175 (2011) 260–270.
- [46] P.J. Ross, *Taguchi Techniques for Quality Engineering*, McGraw-Hill, New York, 1996.
- [47] C. Xinyu, M.F. Hossain, C. Duan, J. Lu, Y.F. Tsang, M.S. Islam, Y. Zhou, Isotherm models for adsorption of heavy metals from water – a review, *Chemosphere*, 307 (2022) 135545, doi: 10.1016/j.chemosphere.2022.135545.
- [48] A.A. Sherlala, A.A. Raman, M.M. Bello, A. Asghar, A review of the applications of organo-functionalized magnetic graphene oxide nanocomposites for heavy metal adsorption, *Chemosphere*, 193 (2019) 1004–1017.
- [49] M. Bilal, I. Ihsanullah, M. Younas, M.U.H. Shah, Recent advances in applications of low-cost adsorbents for the removal of heavy metals from water: a critical review, *Sep. Purif. Technol.*, 278 (2021) 119510, doi: 10.1016/j.seppur.2021.119510.
- [50] J.N. Edokpayi, J.O. Odiyo, T.A.M. Msagati, E.O. Popoola, A novel approach for the removal of lead(II) ion from wastewater using mucilaginous leaves of *Diceriocaryum eriocarpum* plant, *Sustainability*, 7 (2015) 14026–14041.
- [51] A.K. Priya, V. Yogeshwaran, S. Rajendran, T.K. Hoang, M.S.-M. Soto-Moscoseo, A.A. Ghfar, C. Bathula, Investigation of mechanism of heavy metals ( $\text{Cr}^{6+}$ ,  $\text{Pb}^{2+}$  &  $\text{Zn}^{2+}$ ) adsorption from aqueous medium using rice husk ash: kinetic and thermodynamic approach, *Chemosphere*, 286 (2022) 131796, doi: 10.1016/j.chemosphere.2021.131796.
- [52] Bonilla-Petriciolet, D.I. Mendoza-Castillo, H.E. Reynel-Ávila, Eds., *Adsorption Processes for Water Treatment and Purification*, Springer International Publishing, Switzerland, 2017.
- [53] J. Wang, X. Guo, Adsorption isotherm models: classification, physical meaning, application and solving method, *Chemosphere*, 258 (2020) 127279, doi: 10.1016/j.chemosphere.2020.127279.
- [54] K.G. Bhattacharyya, A. Sharma, Adsorption of Pb(II) from aqueous solution by *Azadirachta indica* (neem) leaf powder, *J. Hazard. Mater.*, 113 (2004) 97–109.
- [55] A.A. Sherlala, A.A. Raman, M.M. Bello, A. Buthiyappan, Adsorption of arsenic using chitosan magnetic graphene oxide nanocomposite, *J. Environ. Manage.*, 246 (2019) 547–556.
- [56] C.W. Oo, M.J.N. Kassim, A.L. Pizzi, Characterization and performance of *Rhizophora apiculata* mangrove polyflavonoid tannins in the adsorption of copper(II) and lead(II), *Ind. Crops Prod.*, 30 (2009) 152–161.
- [57] A. Khokhar, Z. Siddique, Misbah, Removal of heavy metal ions by chemically treated *Melia azedarach* L. leaves, *J. Environ. Chem. Eng.*, 3 (2015) 944–952.
- [58] X. Tao, L. Xiaoqin, Peanut shell activated carbon: characterization, surface modification and adsorption of  $\text{Pb}^{2+}$  from aqueous solution, *Chin. J. Chem. Eng.*, 16 (2008) 401–406.
- [59] Y. Nuhoglu, Z. Ekmekyapar Kul, S. Kul, Ç. Nuhoglu, F. Ekmekyapar Torun, Pb(II) biosorption from the aqueous solutions by raw and modified tea factory waste (TFW), *Int. J. Environ. Sci. Technol.*, 18 (2021) 2975–2986.
- [60] M. Sener, D.H.K. Reddy, B. Kayan, Biosorption properties of pretreated sporopollenin biomass for lead(II) and copper(II): application of response surface methodology, *Ecol. Eng.*, 68 (2014) 200–208.
- [61] J. Anwar, U. Shafique, Waheed-uz-Zaman, M. Salman, A. Dar, S. Anwa, Removal of Pb(II) and Cd(II) from water by adsorption on peels of banana, *Bioresour. Technol.*, 101 (2010) 752–1755.
- [62] H. Çelebi, O. Gök, Evaluation of lead adsorption kinetics and isotherms from aqueous solution using natural walnut shell, *Int. J. Environ. Res.*, 11 (2017) 83–90.
- [63] T. Kanjilal, S. Babu, K. Biswas, C. Bhattacharjee, S. Datta, Application of mango seed integuments as bio-adsorbent in lead removal from industrial effluent, *Desal. Water Treat.*, 56 (2015) 1–13.
- [64] S. Ravulapalli, R. Kunta, Removal of lead(II) from wastewater using active carbon of *Caryota urens* seeds and its embedded calcium alginate beads as adsorbents, *J. Environ. Chem. Eng.*, 6 (2018) 4298–4309.

Supporting information

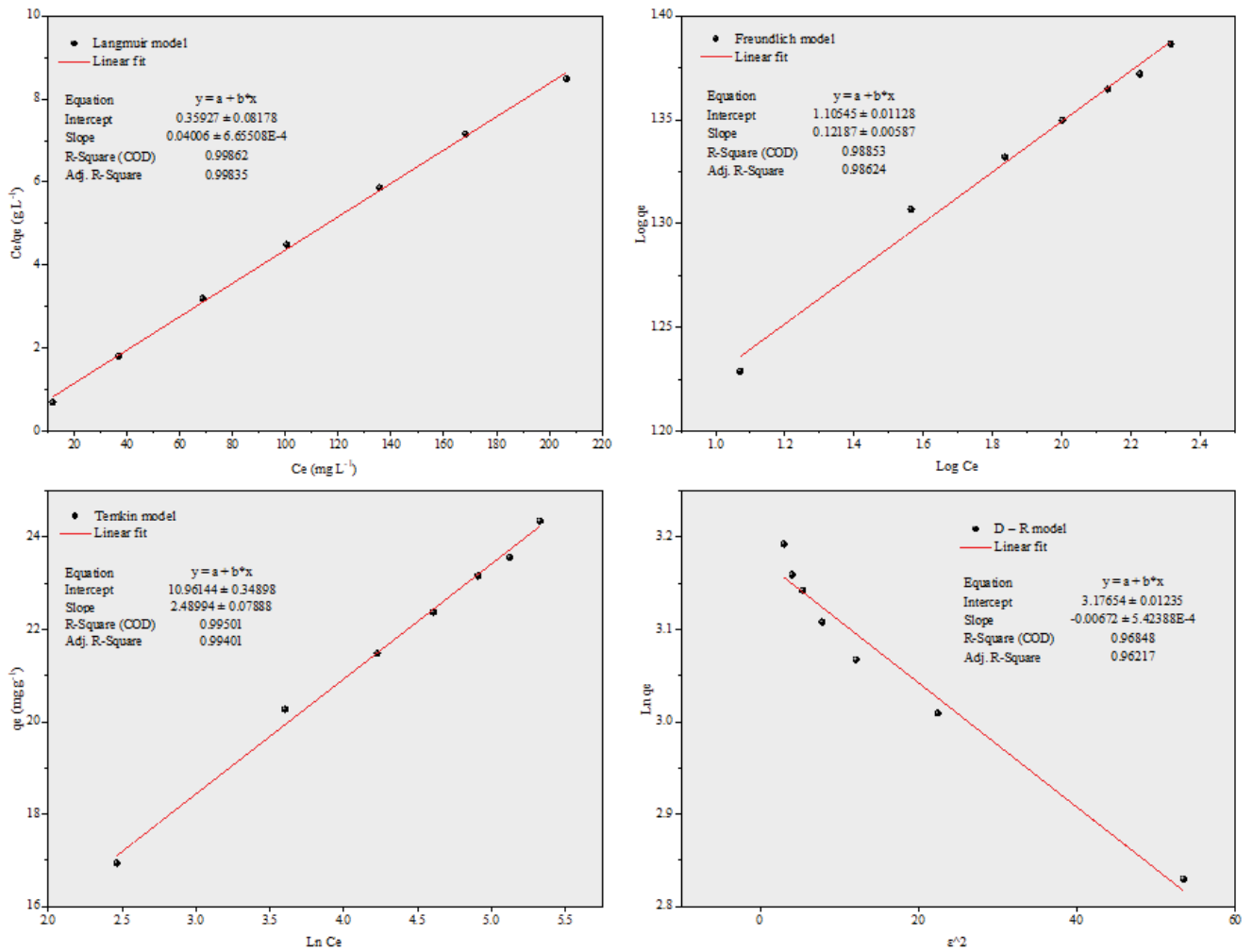


Fig. S1. Linearized equation graphs for the isotherm models.

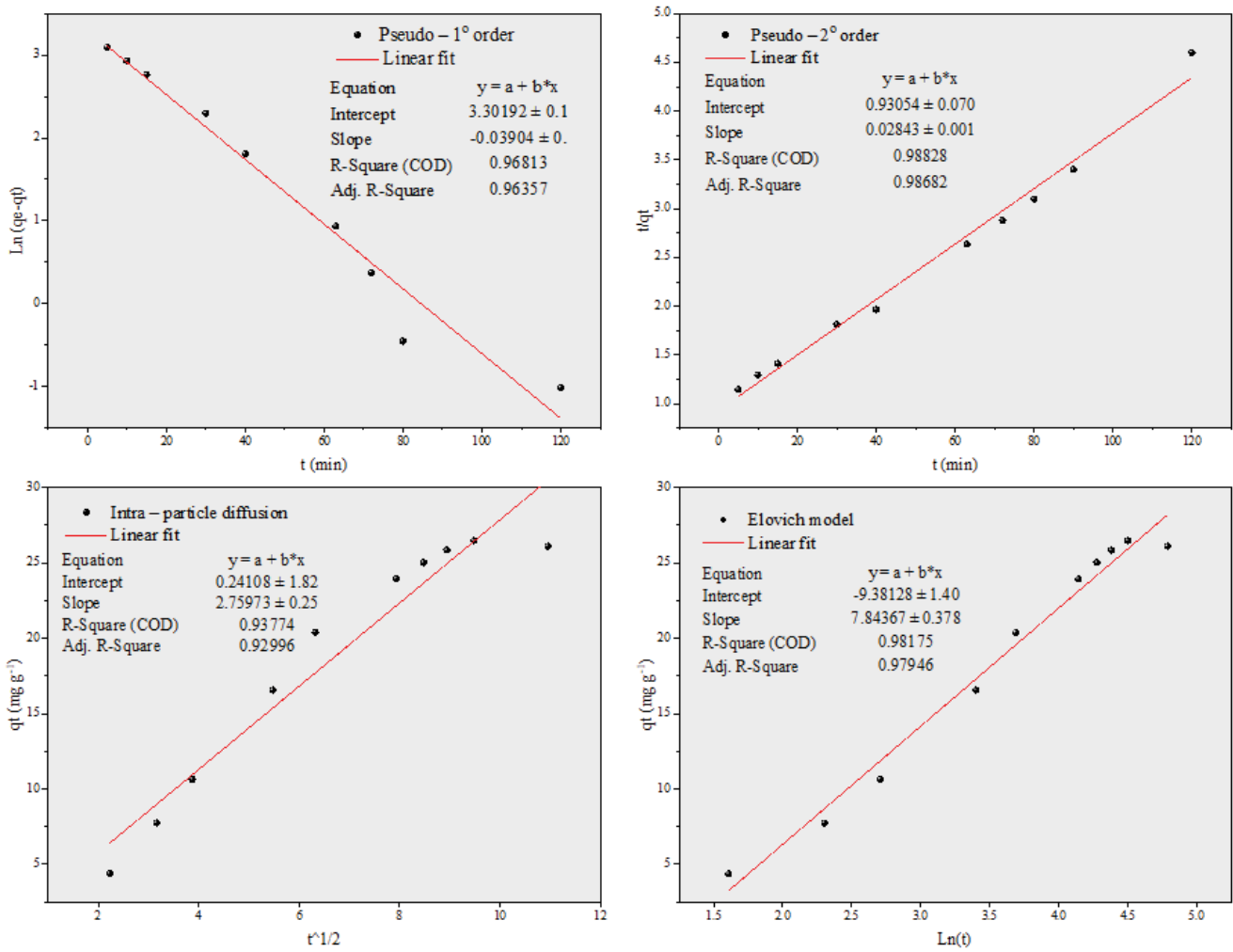


Fig. S2. Linearized equation graphs for the kinetic models.